

ELECTROSTATICALLY COUPLED MICROMECHANICAL BEAM FILTERS

Siavash Pourkamali, Reza Abdolvand, Gavin K. Ho and Farrokh Ayazi

School of Electrical and Computer Engineering
 Georgia Institute of Technology, Atlanta, GA 30332-0250, USA
 Email: siavash@ece.gatech.edu; Tel: 1-404-385-4306; Fax: 1-404-894-5028

ABSTRACT

This paper presents a new electrical coupling technique for implementation of high-order narrow-bandwidth programmable bandpass filters using micromechanical resonators. The concept of electrostatic coupling of closely-spaced microresonators for filter synthesis is introduced and its electromechanical modeling is presented. The electrostatic coupling approach eliminates the need for any physical coupling element in between the resonators and provides the highest degree of tunability and design flexibility among the available filter synthesis approaches. Low frequency single crystal silicon prototypes of second order electrostatically coupled filters have been successfully implemented and characterized. Filter quality factors as high as 6,800 (0.015%BW) with more than one decade of bandwidth tunability are demonstrated in a second order electrostatically coupled beam filter with a center frequency of 170kHz.

1. INTRODUCTION

High performance integrated micromechanical filters can find numerous applications as frequency-selective components in low-power microsystems. High order bandpass characteristics are typically achieved by coupling individual microresonators to each other. Mechanical coupling techniques have been traditionally used for implementation of high order filters in micro and macro domain [1-3].

As the micromechanical resonators are reduced in size to reach higher frequencies, mechanical coupling of individual resonators may require very small coupling elements (e.g., submicron in width wires) that are difficult to implement reproducibly using low-cost manufacturing processes. In MEMS'03, we introduced the concept of electrical coupling of micromechanical resonators for filter synthesis using electrical components (i.e., passive capacitors or active buffers) [4]. Passive electrical coupling of microresonators using shunt capacitors has a greater potential for extension into the ultra high frequency (UHF) range, and provides superior tunability and design flexibility compared to the mechanical coupling technique.

In this work, we present a new passive electrical coupling approach for filter synthesis that does not require distinct electrical components. In this approach, an electrostatic force between the resonating bodies of two closely-spaced microresonators causes coupling and results in a higher order resonant system, without the need for any physical coupling element. Compared to the previously reported capacitive

coupling approach [4], the electrostatic coupling provides even more tunability and design flexibility and alleviates some of the problems associated with capacitive coupling (such as DC biasing of the coupling capacitor).

2. ELECTROSTATIC COUPLING CONCEPT

Figure 1 shows the schematic diagram of an electrostatically coupled beam filter array comprised of a number of resonators separated by small coupling gaps in between.

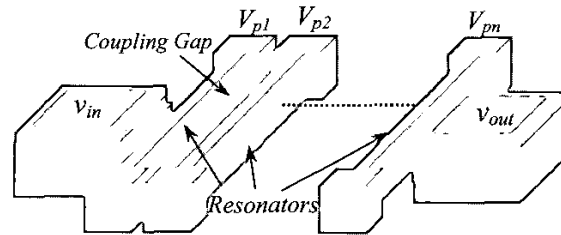


Fig. 1. Schematic diagram of an electrostatically coupled beam filter array.

The difference in the DC polarization voltages (V_p) applied to the adjacent resonators results in an electrostatic force between them. Assume two closely spaced clamped-clamped beam resonators biased at different polarization voltages. For analytical derivation of the coupling strength between the two resonators, each beam is divided into small elements of length dx , as shown in Fig. 2. The electrostatic force in between each pair of corresponding adjacent elements on the two beams is expressed by:

$$df_c = \frac{\partial dE_c}{\partial y} = \frac{1}{2} (\Delta V_p)^2 \frac{\partial dC_c}{\partial y} \quad (1)$$

where df_c is the electrostatic coupling force between the two elements, dE_c is the energy stored in the capacitor between the two elements, y is the total displacement of the elements towards each other along the resonators vibration axis, ΔV_p is the difference between the two polarization voltages applied to the resonators, and dC_c is the value of the coupling capacitor in between the two elements. Each pair of adjacent elements can be considered as a parallel plate capacitor in which the interelectrode gap spacing changes due to the vibrations of the resonators. Assuming small vibration amplitudes, $\frac{\partial dC_c}{\partial y}$ is given by:

$$\frac{\partial dC_c}{\partial y} \approx \frac{dC_{co}}{g_c} \left(1 + \frac{y}{g_c}\right) \quad (2)$$

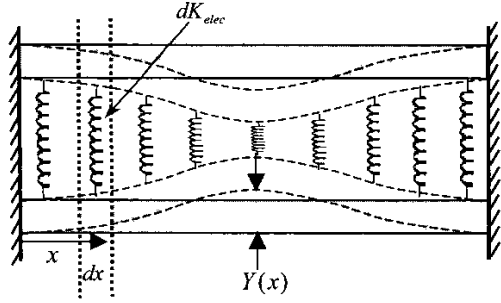


Fig. 2. Schematic diagram of two electrostatically coupled clamped-clamped beam resonators.

where g_c is the coupling gap size in between the resonators, and dC_0 is the rest value of dC_c . Therefore, the electrostatic force can be expressed as:

$$df_c = \frac{1}{2} \frac{dC_{d0} (\Delta V_p)^2}{g_c} \left(1 + \frac{y}{g_c} \right) \quad (3)$$

According to Eq. 3, the electrostatic force has a position dependent component (in addition to its constant component) that is in-phase with the displacement of the resonators towards each other. On the other hand, the force applied by the mechanical stiffness of the structure has a 180° phase shift with the displacement of the resonators. Hence, the position dependent electrostatic force can be modeled as a negative stiffness between the two elements. The electrostatic negative stiffness that exists between every two adjacent elements (represented by springs in Fig. 2) is therefore expressed by:

$$dK_{elec} = -\frac{\partial df_c}{\partial y} = -\frac{(\Delta V_p)^2 \epsilon h_r dx}{g_c^3} \quad (4)$$

where h_r is the height of the resonators and ϵ is the permittivity of the surrounding environment. This effect is similar to the electrostatic frequency tuning of parallel plate resonators where each electrode adds a negative electrical stiffness to the resonator, reducing its resonant frequency.

3. ELECTROMECHANICAL MODELING

Similar to mechanical coupling where the resonators are mechanically connected with compliant mechanical elements, the electrostatically coupled beam resonators are coupled by an electrostatic negative stiffness distributed along their length. In order to develop a lumped-element mechanical equivalent model for the electrostatically coupled beam filter, the overall effective contribution of all the partial stiffnesses between the beams should be calculated.

The effective mechanical stiffness of a beam resonator is a function of the position along the beam length [3]:

$$K_{mech,eff}(x) = \frac{K_{mech,mid}}{Y(x)^2} \quad (5)$$

where $K_{mech,eff}(x)$ is the effective mechanical stiffness at position x , $K_{mech,mid}$ is the mechanical stiffness of the beam in the middle position, and $Y(x)$ is the normalized mode shape function for the first flexural mode of a clamped-clamped beam resonator.

The degree to which each element of the electrostatic stiffness can contribute to the frequency response depends inversely on the effective mechanical stiffness at the element location. The larger the effective mechanical stiffness is, the weaker the effect of electrostatic stiffness on the resonator frequency is at that location. Therefore:

$$dK_{elec,eff}(x) = Y(x)^2 dK_{elec} \quad (6)$$

In order to define an overall effective electrostatic stiffness with respect to the middle position in the beam, the effective electrical stiffnesses at all points along the beam should be added:

$$K_{elec,eff} = \int_0^L Y(x)^2 dK_{elec} = -\frac{\epsilon h_r (\Delta V_p)^2}{g_c^3} \int_0^L Y(x)^2 dx \quad (7)$$

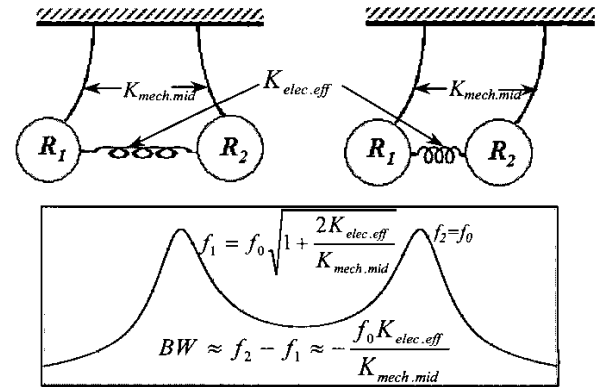


Fig. 3. Equivalent lumped element model of a second order electrostatically coupled filter and its frequency response.

Figure 3 shows the mechanical equivalent lumped element schematic of a second order electrostatically coupled filter and its frequency response. Unlike the mechanically coupled filters where the resonators move in-phase in the first resonant mode and out-of-phase in the second resonant mode, the resonators are out-of-phase in the first mode of an electrostatically coupled filter, and vice versa. This stems from the fact that the electrostatic coupling spring has a negative effective value and reduces the stiffness of the resonator causing a lower frequency resonant mode when interfering with the resonators (in their out-of-phase motion).

In contrast to the mechanical coupling approach where the coupling strength and consequently the filter bandwidth is determined only by the stiffness and position of the coupling element, the coupling strength in electrostatically-coupled arrays is a function of the polarization voltages and geometrical parameters, i.e., the coupling area and gap

spacing. Therefore, characteristics of electrostatically-coupled filters can be tuned/programmed by changing the polarization voltages to reach the target specifications.

To derive an electrical equivalent circuit for the electrostatically-coupled filters, the following conversions from the mechanical to the electrical domain should be performed:

$$\begin{aligned} \text{displacement } (y) &\rightarrow \text{current } (i) \\ \text{force } (f) &\rightarrow \text{time derivative of voltage } (\partial v / \partial t) \end{aligned}$$

so that stiffness is converted to the inverse of capacitance, mass to inductance, and damping to resistance. The resonator is then represented by a series RLC tank. The force applied by the coupling stiffness is determined by the sum of the displacements of the resonators. Therefore, the coupling element will be presented by a parallel negative capacitor to ground at the coupling node in between the two resonators so that the sum of the currents of the resonators will determine the voltage of the coupling capacitor.

Based on the above discussion, the electrical equivalent circuit for a second order electrostatically coupled is as shown in Fig. 4. The value of the series capacitor of the resonators (C_{io}) depends on the mechanical properties of the resonators (mass and stiffness) as well as the electromechanical coupling strength between the input and output electrodes and the resonating body. The electromechanical coupling in turn depends on the applied polarization voltages and the capacitive gap between the electrodes and the resonators, as well as the electrode area. Therefore:

$$C_{io} = \frac{1}{R_{io}Q\omega_0} = \frac{C_{so}C_{do}V_{p1}V_{p2}}{\sqrt{K_{mech}M\omega_0g_dg_s}} \quad (8)$$

where, R_{io} is the equivalent resistance of the resonators, Q is the mechanical quality factor of the resonators, C_{so} and C_{do} are the sense and drive electrode capacitances respectively, g_d and g_s are the sense and drive capacitive gap sizes, M is the equivalent mass of the resonators, and ω_0 is the operating angular frequency of the resonators.

Since the capacitor values are inversely proportional to the stiffness that they represent, the value of the coupling capacitor will be:

$$C_c = \frac{C_{io}K_{mech}}{K_{elec,eff}} \quad (9)$$

The two terminating transformers count for any asymmetry between the input and output ports of the filter which results in different impedance levels at the input and output ports and their transformation coefficients are:

$$T_{oi} = \frac{g_s A_d V_{p1}}{g_d A_s V_{p2}} = T_{io}^{-1} \quad (10)$$

Capacitors C_i and C_o at the input and output nodes, represent the physical pad and sense or drive capacitors existing at the input and output of the filter.

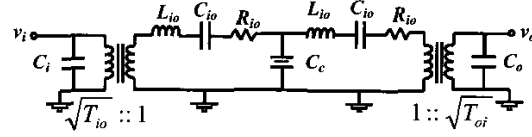


Fig. 4. Electrical Equivalent circuit of a second order electrostatically coupled filter.

4. SILICON IMPLEMENTATION

For practical demonstration of the electrostatic coupling concept, single crystal silicon resonators with lithographically defined coupling and transducer gaps (1-3 μ m wide) were fabricated on SOI substrates using a single mask fabrication process consisting of etching high aspect ratio trenches in the SOI device layer to the buried oxide followed by an undercut in HF. Figure 5 shows the SEM view of a fabricated second order beam filter. The filter is comprised of two 15 μ m thick, 5 μ m wide, 500 μ m long clamped-clamped beam resonators with a 2.8 μ m wide coupling gap in between.

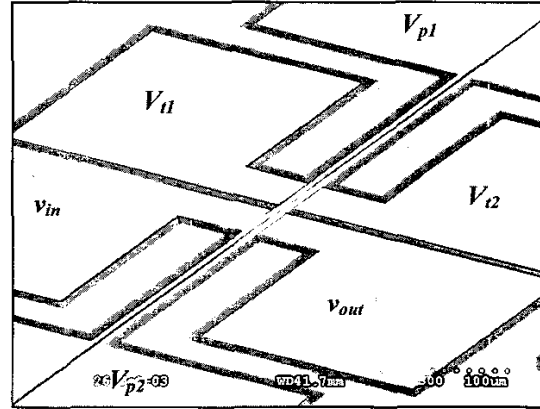


Fig. 5. SEM of a fabricated second order clamped-clamped electrostatically coupled beam filter.

The fabricated filters were tested under vacuum in a custom vacuum chamber. As shown in Fig. 5, the sense and drive electrodes are split in two sections so that tuning voltages (V_i) can be applied to one of the sections to adjust the resonant frequencies of the resonators to equal values while different polarization voltages are applied to them. However due to fabrication deficiencies and slight frequency mismatch between the coupled beams, the resonators can have equal center frequencies while different polarization voltages are applied to provide electrostatic coupling. In case of completely matched resonators and lack of split electrodes, application of equal polarization voltages with opposite polarities can provide the desired electrostatic coupling.

Figure 6 shows the frequency responses taken from the filter of Fig. 5 with different sets of applied polarization voltages. Quality factor of individual resonators was measured to be 30,000. As the polarization voltages

increase, the frequency tuning slope increases and the required polarization voltage difference to compensate for the frequency mismatch of the beams will be smaller, resulting in a weaker coupling and smaller filter bandwidth. Resonance peak separations ranging from 200Hz to 24Hz (a bandwidth tunability of close to one decade) was achieved for this filter by changing the polarization voltages (Fig. 6). Filter Q of 6800, 40 dB shape factor of 12.5, and stopband rejection of higher than 50dB has been achieved for the 24Hz bandwidth filter of Fig. 6. Such high filter quality factors can not be easily achieved for the mechanically coupled filters unless ultra-compliant mechanical coupling elements are used.

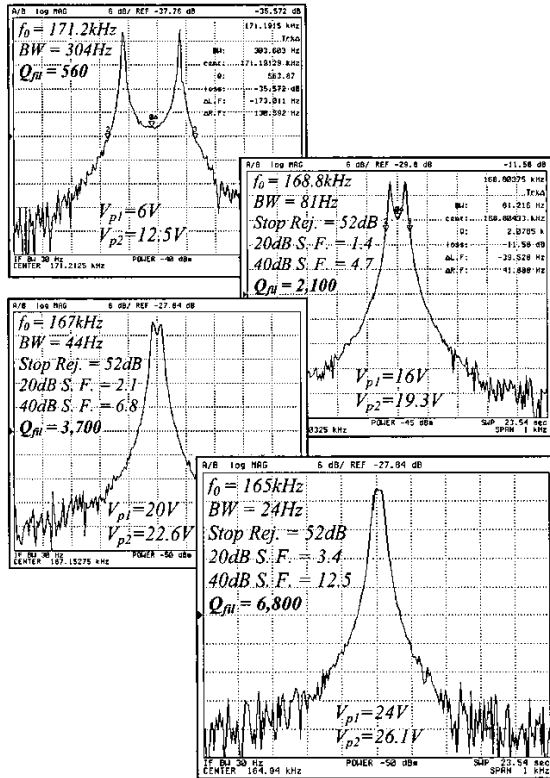


Fig. 6. Frequency response of the electrostatically coupled filter of Fig. 5 with different sets of polarization voltages applied to the beams.

Due to existence of large pad capacitors at the input and output of the device, it was not possible to damp the resonators and flatten the passband by adding resistive terminations.

Resonance peak separation versus the square of the polarization voltage difference (ΔV_p^2) for the same filter is plotted in Fig. 7. As it is predicted by Eq. 7, the equivalent electrostatic stiffness and consequently the frequency difference between the two resonance modes of the filter is a linear function of the square of polarization voltage difference. The measured bandwidth tuning slope of 4.7

Hz/V² is in good agreement with the calculated value of 4.9 Hz/V² obtained through Eq. 7.

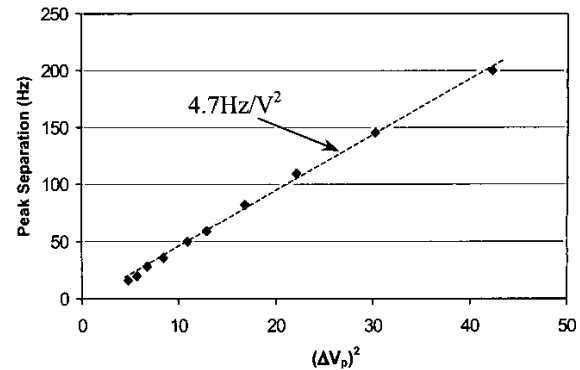


Fig. 7. Resonance peak separation versus the square of polarization voltage difference (ΔV_p^2) for the electrostatically coupled filter of Fig. 5.

5. CONCLUSION

A new filter synthesis technique based on electrostatic interaction of closely-spaced resonators was introduced. The concept of electrostatic coupling and its theoretical derivations were presented. The described coupling technique does not require any physical coupling elements for implementation of coupled arrays of resonators. It was analytically and practically shown that the electrostatically coupled filter can be programmed after fabrication to have the desired specifications. In addition, compared to mechanically coupled filters, much higher filter quality factors can be achieved in electrostatically-coupled filters. Measurement results of a 170kHz second order electrostatically coupled filter showed filter quality factors as high as 6,800 and more than 10 times of bandwidth tuning. The same coupling technique can be applied to ultra-stiff bulk-mode resonators for higher frequency operation.

Acknowledgements

This work was supported by DARPA under contract # DAAH01-01-1-R004. Authors would like to thank the staff at the Georgia Tech Microelectronics Research Center for their assistance.

REFERENCES

- [1] A.-C. Wong, et al, "Anneal-activated, tunable, 68MHz micromechanical filters", Sensors and Actuators 99, 1390-1393.
- [2] D. S. Greywall, et al, "Coupled micromechanical drumhead resonators with practical applications as electromechanical bandpass filters", J. Micromech. Microeng. 12 (2002) 925-938.
- [3] R. A. Johnson, "Mechanical filters in electronics", A Wiley-interscience publication.
- [4] S. Pourkamali, et al. , "A 600kHz electrically coupled MEMS bandpass filter", MEMS'03, pp. 702-705.